

Bayesian spatio-temporal model with INLA for dengue fever risk prediction in Costa Rica

Shu-Wei Chou-Chen ^{*}, Luis A. Barboza, Paola Vásquez, Yury E. García,
Juan G. Calvo, Hugo G. Hidalgo, Fabio Sanchez

February 15, 2023

Abstract

Due to the rapid geographic spread of the *Aedes* mosquito and the increase in dengue incidence, dengue fever has been an increasing concern for public health authorities in tropical and subtropical countries worldwide. Significant challenges such as climate change, the burden on health systems, and the rise of insecticide resistance highlight the need to introduce new and cost-effective tools for developing public health interventions. Various and locally adapted statistical methods for developing climate-based early warning systems have increasingly been an area of interest and research worldwide. Costa Rica, a country with micro-climates and endemic circulation of the dengue virus (DENV) since 1993, provides ideal conditions for developing projection models with the potential to help guide public health efforts and interventions to control and monitor future dengue outbreaks.

Keywords: Public Health, Bayesian inference, spatio-temporal models, climate, vector-borne disease

1 Introduction

Dengue is one of the most prevalent vector-borne diseases globally, affecting individuals of all ages. The infection can be asymptomatic or cause a broad spectrum of clinical manifestations that range from a non-specific and auto-limited viral syndrome to a disease with hemorrhagic manifestations and multi-systemic damage that can lead to the death of the patient [1]. The infection is caused by one of four dengue virus serotypes (DENV 1–4) transmitted to humans through the bite of infected female mosquitoes, primarily by *Aedes aegypti* and *Aedes albopictus* as a secondary vector.

The interaction of a variety of factors, including globalization, trade, travel, demographic trends, and warming temperatures, have been associated with the spread of the mosquito, which is now present on all continents except Antarctica [2, 3], making it one of the 100 worst invasive species in the world [4]. It has also led to the emergence of the disease in places where it was previously absent [5, 6, 7, 8, 9], putting more than half of the world’s population at risk of infection, mainly in tropical and subtropical regions [1]. In this context, and without effective prevention and control measures, dengue is expected to continue its geographical expansion [10, 11]. Due to the lack of a vaccine and antiviral drugs, the key to preventing and

^{*}corresponding author: shuwei.chou@ucr.ac.cr

controlling outbreaks continues to be the reduction of breeding sites through chemical and biological interventions as well as the active involvement of the community, which is mainly dependent on available resources of the affected countries.

Given that the ecology of the virus is intrinsically tied to the ecology of mosquitoes that transmit dengue [12], climatic and environmental conditions can alter spatial and temporal dynamics of vector ecology, especially temperature, rainfall, and relative humidity [13, 14]. Temperature affects viral amplification [15], increases vector survival, reproduction, and biting rate [16, 17]. Long-term breeding habitats for eggs, larvae, and pupae may be influenced by wastewater left by rainfall or human behavior of storing water in containers [18, 19]. Dengue incidence has also been associated with vegetation indices, tree cover, housing quality, and surrounding land cover [20, 21].

Understanding the influence of these climatic variables on disease incidence in different regions can lead to early detection of disease progression, guide resource allocation, and implement appropriate health intervention [1]. In this effort, several methods of surveillance systems have been developed [22, 23, 24]. However, successful early warning strategies are limited due to the complex and dynamic nature of the disease. The complex interaction of biological, socioeconomic, environmental, and climatic factors creates substantial spatio-temporal heterogeneity in the intensity of dengue. It imposes a challenge in the creation of surveillance and control systems.

In Costa Rica, a Central American country with a variety of micro-climates in an area of $51,179 \text{ km}^2$, dengue has been endemic since 1993 and has represented a public health burden since then. According to the Ministry of Health, more than 398,000 cases have been reported during the last 28 years [25]. DENV-1, DENV-2, and DENV-3 have been the main serotypes in circulation. However, it is essential to highlight that in 2022 the circulation of serotype four was identified in different municipalities in the country. Since this serotype has historically been absent in national territory, its emergence and lack of immunity in the country which can lead to an increase in the incidence of cases reinforces the need to increase prevention, detection, and timely treatment efforts and thus avoid an increase in the incidence and evolution of more severe forms of the disease.

In this work, we propose a spatio-temporal model to predict dengue in Costa Rica, including climatic variables and geographic information to capture the effect of factors that modulate the spatio-temporal variation of dengue incidence in the country and whose information is not available, such as population mobility, socioeconomic and demographic information. This study is part of a series of efforts [26, 27], which have been carried out to develop an early warning system to monitor dengue risk in the country. The aim is to provide guidance tools to the health authorities of Costa Rica that can be implemented and validated and to optimize and distribute resources in the prevention and control of dengue.

Based on dengue’s historical incidence burden and suitable environment for disease transmission, the Costa Rican health authorities have identified 32 municipalities of interest (out of the 83 municipalities the country is divided) where the study was conducted. The selection included mainly municipalities located in the coastal areas on the Pacific and Caribbean coasts and municipalities in the Great Metropolitan Area, the country’s most urban and populated region. This selection was also based on the decision-makers necessity to include new and cost-effective tools to guide the allocation of resources throughout the year. The article is divided as follows: Section 2 describes the data, statistical model, assumptions, and implemented methodologies. Section 3 presents the results for the 32 municipalities of interest. Finally, section 4 discusses this modeling approach’s results, limitations, advantages, and

future work.

2 Methods

2.1 Data description

2.1.1 Dengue Cases

For this analysis, we used monthly dengue cases for 32 municipalities of interest to public health authorities in Costa Rica. The data covered 2000-2021 obtained from the Ministry of Health of Costa Rica [28].

2.1.2 Climate variables

1. Daily Precipitation estimates ($P_{i,t}$) were used to index land surface rainfall. Data were obtained from the Climate Hazards Group InfraRed Precipitation with Station data (CHIRPs); see [29]. Due to the high-resolution spatial nature of this dataset (5km by 5km), we were able to compute monthly cumulative rainfall estimates for each municipality by adding the exact estimate over smaller administrative areas (*distritos*).
2. El Niño Southern Oscillation (ENSO, $S_{i,t}$) variations were indexed using the Sea Surface Temperature Anomaly (SSTA) index for the region known as Niño 3.4 (5N-5S, 120W-170W). monthly data was obtained from the Climate Prediction Center (CPC) of the United States National Oceanographic and Atmospheric Administration (NOAA) (see [30]).
3. Normalized Difference Vegetation Index (NDVI, $N_{i,t}$), an index of the greenness of vegetation for a 16-day time resolution and 250m spatial resolution. It was obtained from the Moderate Resolution Imaging Spectroradiometer (MODIS) satellite and available through the `MODISTools` R package (see [31]).
4. Daytime Land Surface Temperature (LST, $L_{i,t}$) in degrees Kelvin for an 8-day time resolution and 1km spatial resolution were obtained using the same resources as the NDVI covariate.
5. Tropical Northern Atlantic Index (TNA, $TN_{i,t}$). Anomaly index of the Sea-Surface Temperature Anomaly (SSTA) over the eastern tropical North Atlantic Ocean (see [32]). Previous work in the region [33] suggested that including SSTA information from the Caribbean/Atlantic improves the performance of the prediction of land surface precipitation and temperature in Central America compared to forecasts produced with only Pacific Ocean ENSO conditions.

2.2 Model

We incorporate the historical exposure of the climate covariates and the behavior of the relative risks in the past by applying the Distributed Lag Non-Linear Model (DLNM) framework [34, 35]. This methodology incorporates a bi-dimensional space of functions that specifies an exposure-lag-response function $f \cdot w(x, l)$, which depends on the predictor x along the time lags l in a combined way. This combination specifies a non-linear and delayed association

between a climate covariate and dengue incidence. For each covariate, we consider a minimum of 3-month lag and a maximum exposure of 12 months to obtain the estimates up to a maximum of a three-month ahead prediction. This combination of lags was determined based on the cross-correlation and wavelet behavior among the series (see [27]). We also tested the model with different combinations of maximum and minimum lags.

To compare the predictive gain of the non-linear specification against the linear ones, we compared models with a non-linear relationship of the delayed effect of exposure on the outcome using natural cubic B-splines function with 2 knots for each covariate and delayed effects against models with the linear relationship of the delayed effect of exposure on the outcome.

After specifying the historical exposure of the covariates, we use a spatio-temporal Bayesian hierarchical model with the response variable as the monthly number of cases of dengue fever for each municipality $i, i = 1, \dots, 32$ for $t = 1, \dots, 264$ as follows:

$$Y_{it} | \mu_{it}, \kappa \sim \text{NegBin}(\mu_{it}, \kappa), \quad (1)$$

$$\log(\mu_{it}) = \log(E_{it}) + \log(RR_{it}), \quad (2)$$

and

$$\log RR_{it} = \alpha + f_1(RR_t) + f_2(P_t) + f_3(S_t) + f_4(N_t) \\ + f_5(L_t) + f_6(TN_t) + f_7(M_t) + \phi_{i,(month)} + \theta_{i,(year)},$$

where $f_k, k = 1, \dots, 7$ is the exposure-lag-response function that applies a linear effect on each climate covariate from lag 3 to 12; $\phi_{i,(month)}$ is the municipality-specific monthly random effect that follows a prior according to a cyclic random walk of order 1, i.e., $\phi_{i,(month)} - \phi_{i,(month-1)} \sim N(0, \sigma_\phi^2)$; and $\theta_{i,(year)}$ is a random spatial effect.

For the spatial effect, two types of proximity matrix \mathbf{W} are defined:

1. The usual neighbor matrix is defined by $\mathbf{W} = \{\mathbf{W}\}_{ij} = 1$ if municipality i and j are neighbors, and 0 otherwise.
2. An alternative distance matrix based on the main road distance in kilometers between the central downtown of each pair of municipalities, i.e. $\mathbf{W} = \{\mathbf{W}\}_{ij} = 1$ if the distance is less than its overall median and 0 otherwise. We incorporate this distance to provide a more realistic way to measure the proximity between social dynamics.

Four types of spatial structures are implemented. First, the independent case is assumed. Then, we used the intrinsic conditional auto-regressive (CAR) specification with improper prior, the CAR model with proper prior, and also the Besag-York-Mollie (BYM) model [36].

Specifically, the CAR specification for the spatial effect for a specific year is defined by:

$$\theta_{i,(year)} | \theta_{j,(year), \tau_\theta} \sim N \left(\frac{1}{n_i} \sum_{j \sim i} \theta_{j,(year)}, \frac{1}{\tau_\theta n_i} \right),$$

where τ_θ is the conditional precision, $j \sim i$ denotes that $\mathbf{W}_{ij} = 1$, and n_i is the numbers of neighbors, according to the definition of the two types of proximity matrix. The proper CAR model is obtained by adding a positive quantity d to n_i , whereas the BYM model is obtained by adding an unstructured random effect per municipality. For more details, see [37]. The R packages `dlnm` [38] and `INLA` [39] were used for all calculations.

Finally, we performed two simple forecasting procedures to compare them with the proposed model in terms of predictive skill. Both methods use the training set for the last five years (2015-2019). First, naïve forecasting is performed using a simple monthly mean \overline{RR}_{it} for the last five years. This method is easy to compute, but the prediction interval can only be calculated by assuming strong assumptions, such as independence; thus, only $NMRSE$ can be computed.

Second, as an alternative, we estimated the model (1) with

$$\log RR_{it} = \alpha,$$

as a Negative Binomial null model so that the prediction uncertainty can be computed in this case. The main objective of performing these two prediction procedures is to compare how the proposed model outperforms these two simple algorithms by using a more complex structure composed of the covariates and spatial random effect.

2.3 Model selection and prediction

Previous studies [27, 40] have shown that these climatic covariates are essential to predict dengue incidence. To begin the calibration, a training period is chosen to fit the model 1 using different combinations of covariates and spatio-temporal configurations of the model. First, the DLNM framework allows us to choose different combinations of maximum and minimum lags of historical information on the covariates. Moreover, the basis was chosen to be nonlinear and linear for all covariates. Finally, four spatial structures were fitted: independent, CAR, proper CAR, and BYM models.

The best model was chosen by comparing all fitted models by different criteria. The deviance information criteria (DIC) and the mean cross-validation (CV) log score are calculated for each model. The DIC is a measure that contemplates the model's precision and complexity. At the same time, the CV log score is a criterion that measures the model's predictive capacity, letting one data out at a time.

Finally, two metrics to compare the predictive performance of each model are computed. The normalized Mean-Squared Error ($NRMSE$):

$$NRMSE = \sqrt{\frac{1}{m\overline{RR}} \sum_{t=1}^m (RR_t - \widehat{RR}_t)^2},$$

where m is the number of months in the testing period, \overline{RR} is the mean relative risk over the same period, and \widehat{RR}_t is the estimated relative risk according to any of the two models. The normalized Interval Score at α level (NIS_α) is the normalized version of the Interval Score (see [41] and [42]):

$$NIS_\alpha = \frac{1}{m\overline{RR}} \sum_{t=1}^m \left[(U_t - L_t) + \frac{2}{1-\alpha} (L_t - RR_t) \cdot 1_{RR_t < L_t} + \frac{2}{1-\alpha} (RR_t - U_t) \cdot 1_{RR_t > U_t} \right],$$

where U_t and L_t are the upper and lower limits of the prediction interval, respectively, the latter metric is more complete in evaluating the models' predictive capacity when the uncertainty is summarized through a predictive interval [42]. It has been used in previous predictive studies on dengue fever in Costa Rica (see [26, 40]). We use the normalized version of RMSE and IS because we can compare different locations regardless of the scale of their relative risk.

3 Results

We fitted the model (1) specifying different structures to the dengue data using all climate covariates. The training period consists of monthly data from January 2000 to December 2020, and the testing period from January 2021 to March 2021.

Regarding the DLNM framework, specifying the maximum and minimum lags to incorporate historical exposure of climate covariates is challenging. We set the maximum and minimum lags as 12 and 3 lags, respectively, so that we can predict the dengue data for up to three months. We also fitted the models using maximum and minimum lags of 12 and 0, respectively, and the difference in predictive precision is insignificant with respect to the first alternative. Table 1 presents all models' DIC and CV log-scores with the smallest values per metric in bold. First, it is clear that, in terms of the goodness of fit, the models with

Table 1: Comparison of the models according to Deviance information criterion (DIC) and mean cross-validation (CV) log-score.

DLNM	Proximity matrix	Spatial structure	DIC	CV log-score
Linear*	Neighbor	Independent	57135.37	3.8710
		CAR	54256.47	3.6872
		proper CAR	52628.40	3.5774
		BYM	52632.24	3.5784
	Distance	CAR	53416.92	3.6264
		proper CAR	52633.29	3.5787
		BYM	52636.92	3.5787
		Non-linear*	Neighbor	Independent
CAR	50640.66			3.6838
proper CAR	49438.81			3.5954
BYM	49461.01			3.5977
Distance	CAR		54674.34	3.9653
	proper CAR		49468.89	3.5985
	BYM		49456.27	3.5971

* The best model for each DLNM specification is marked in bold.

the spatial structure are better than those assuming independent spatial structures. Then, we can see that the differences in DIC and CV log scores are minimal when we compare the linear and non-linear (B-splines) DLNM framework.

Finally, to guarantee an acceptable balance between the complexity of the models and the predictive precision over all the locations using the DIC and CV log-scores, we chose as the best-fitted model the proper CAR model with linear DLNM and with neighbor proximity matrix.

Table 2 summarizes the predictive metrics ($NRMSE$ and $NIS_{0.05}$) of the training and testing periods per municipality for the best model compared to the baseline model with an independent spatial structure.

We can observe how spatial information can contribute to obtaining more precise predictions by comparing those two modeling alternatives. The most noticeable municipality Parrita has a particular behavior. The baseline model with an independent spatial structure

Table 2: Predictive metrics of training and testing data set of the selected model

Municipality	Training set				Testing set			
	Independent		Proper CAR		Independent		Proper CAR	
	<i>NRMSE</i>	<i>NIS</i> ₉₅	<i>NRMSE</i>	<i>NIS</i> _{0.05}	<i>NRMSE</i>	<i>NIS</i> _{0.05}	<i>NRMSE</i>	<i>NIS</i> _{0.05}
Alajuela	0.7815	14.5297	0.3982	5.3710	0.0750	1.0905	0.0416	1.6417
Alajuelita	0.3090	23.2238	0.2175	13.1177	0.4515	22.8135	0.0515	2.0922
Atenas	4.6100	24.7736	2.5706	10.1453	5.1453	87.6173	0.3283	10.2199
Cañas	10.1008	24.3243	5.7069	12.3277	5.8803	60.7800	0.4829	6.8129
Carrillo	4.3786	15.9598	3.5404	9.1421	0.9860	13.2041	0.4175	2.5945
Corredores	5.0620	25.1830	2.5155	8.6126	1.6824	17.0115	0.5697	1.9358
Desamparados	0.2351	18.6300	0.1466	8.2922	0.0282	3.0978	0.0142	3.0085
Esparza	4.7287	17.4775	2.6296	8.4081	1.1899	16.1291	0.1849	2.1748
Garabito	38.4940	29.0191	5.2545	9.8071	28.8475	232.7807	0.4258	12.9528
Golfo	3.7245	23.5563	1.7734	8.2174	2.0078	35.7736	0.3499	8.5601
Guacimo	1.9057	13.8120	1.0844	4.4132	3.0709	18.1805	2.0633	4.8628
La Cruz	6.2484	26.6755	4.2779	14.3090	6.0351	118.6721	0.5029	14.7439
Liberia	3.6829	23.1675	2.0260	10.2626	4.0913	92.4202	0.5693	16.2507
Limon	2.9640	17.1259	1.6025	6.7593	1.3724	11.2322	0.1034	1.7042
Matina	5.1143	19.9086	2.7162	7.4890	58.0750	192.2903	0.1232	3.0869
Montes de Oro	5.9220	21.8260	4.1289	12.2332	11.4909	126.5836	1.2106	19.5139
Nicoya	2.8036	20.5059	2.0672	10.1305	3.6262	101.6524	0.1894	10.2497
Orotina	13.7161	17.5376	4.0681	6.0472	1.0599	6.7613	0.4888	1.5221
Osa	5.9295	33.7053	4.2208	17.2559	1.1235	13.0806	0.5758	1.7891
Parrita	1.24×10^9	24483.9181	13.7622	9.8340	4.4446	46.3670	0.6773	7.9705
Perez Zeledón	2.0103	30.0358	0.8733	9.4268	1.2543	20.3380	0.1783	1.3942
Pococí	2.2524	12.7658	1.3001	6.1328	1.0524	12.0212	0.1284	1.8534
Puntarenas	1.5802	12.8416	0.9303	4.6933	1.3263	23.9665	0.1646	1.7646
Quepos	56.8344	37.6499	10.0908	12.9868	36.9331	257.7509	1.1780	23.2153
San Jose	0.2105	12.6814	0.1328	5.2650	0.0215	1.2409	0.0155	2.3248
Santa Ana	0.7837	21.9311	0.5860	12.6213	0.6759	43.5264	0.3576	15.4854
SantaCruz	35.1198	37.3329	8.4762	12.7070	6.5905	91.5896	0.3027	3.0635
Sarapiquí	7.9218	22.2392	2.8096	6.9807	0.3880	4.9820	0.1047	1.9942
Siquirres	2.1184	13.9371	1.4077	6.6140	2.7214	19.0646	0.3564	1.7977
Talamanca	4.9193	21.1751	2.2374	8.0522	0.1113	0.7642	0.7989	1.3152
Turrialba	2.5905	25.2386	1.9572	15.8268	1.0122	20.0694	0.2614	1.8489
Upala ¹	1.2744	21.7159	0.9203	12.2963	-	-	-	-

¹ *NRMSE* and *NIS*_{0.05} of the testing set for Upala are not shown since the observed relative risks are zero.

cannot predict training and testing periods. In contrast, our selected model with proper CAR spatial structure can substantially reduce its prediction metrics. Moreover, the precision of the proposed model performs better than the simple forecasting procedures (see Table A.1. in Supplementary Material).

Close to Parrita, two municipalities with moderately high predictive metrics are Garabito and Quepos, located on the country's central pacific coast. We suspect that the difficulty of predicting these particular areas is mainly because they are touristic, and dengue cases in these areas are likely underreported.

Besides the climatic covariate's contribution to the model, temporal and spatial random effects ($\phi_{i,(month)}$ and $\theta_{i,(year)}$) are also important factors in modeling dengue behavior because they provide temporal or spatial information which is not observable through the selected covariates. Figure 1 shows the behavior of municipality-specific monthly random effects. Municipalities with similar temporal behavior are identified as Groups 1 to 7, and the last group consists of municipalities that do not have a specific behavior. Later on, the geographic location of these groups of municipalities is illustrated in Figure 2. We observe that the information provided by the temporal random effects mostly agrees with the temporal variation due to the microclimates in the country.

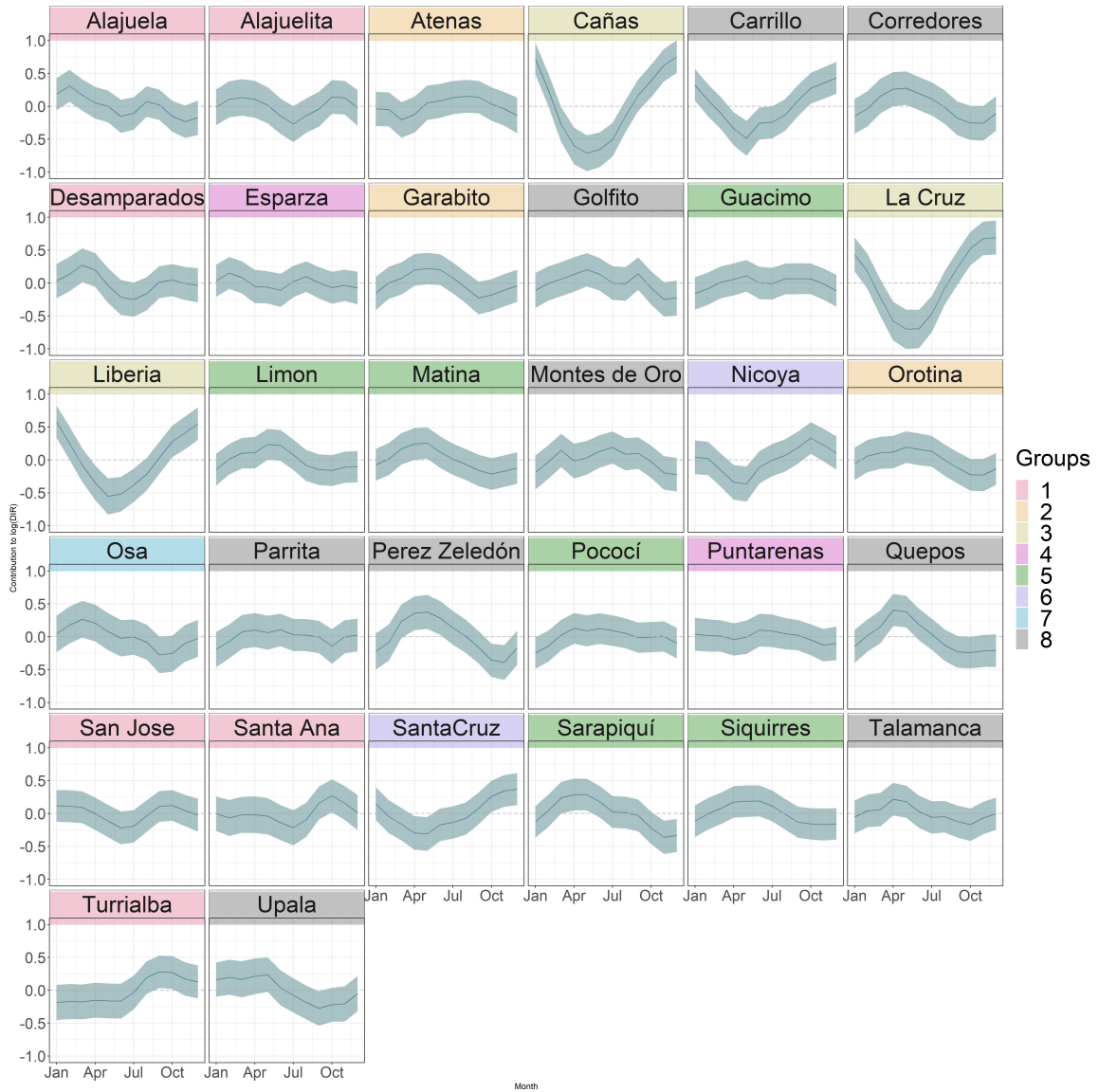


Figure 1: Posterior mean and 95% credible interval of municipality-specific monthly random effects.

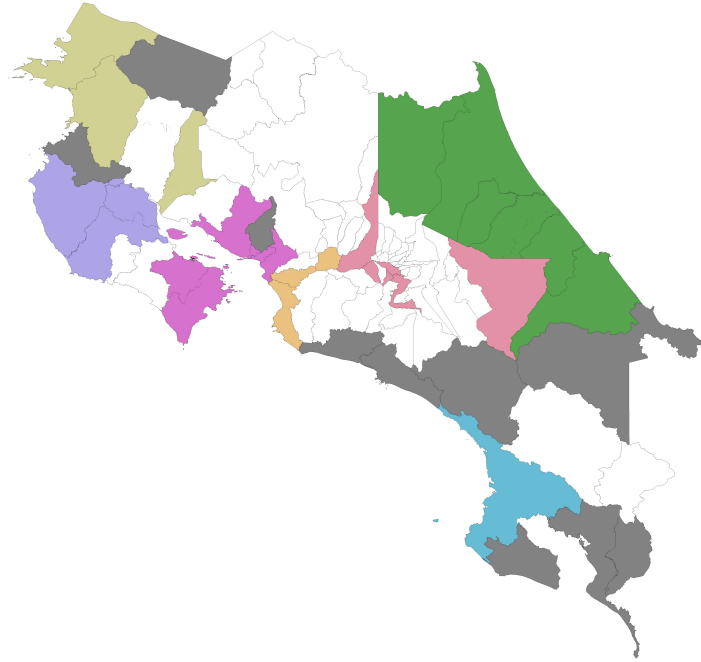


Figure 2: Illustration of eight groups with similar temporal behavior.

On the other hand, the spatial random effect for each year is illustrated in Figure 3. We observe that there are clusters of cantons for different years that present a higher or lower log of relative risk. For instance, the south pacific part of the country in 2002 and the north pacific region presented a lower contribution of log of relative risk, while the central pacific in 2009 presented a high contribution of log of relative risk.

It is important to notice that this spatial random effect is the variation in log of relative risk that is not captured by the climatic covariates. Still, somehow they can be modeled by the neighbor's spatial structure. It is known that dengue is a complex phenomenon that involves not only climatic factors but also socioeconomic components and human mobility. Furthermore, there are also outbreaks in certain municipalities during different periods that are not captured by the climatic covariates in this study. In this way, this model is more complete compared to the baseline model assuming independent spatial structure.

The dengue prediction can be visualized by using temporal or spatial dimensions. For the temporal dimension, Figure 4 shows the 95% posterior predictive dengue relative risk in the training period of the best six municipalities and the three worst municipalities according to $NIS_{0.05}$ during the testing period. In addition, Figure 5 presents the % posterior predictive dengue relative risk of the same municipalities during the testing period. In general, the behaviors of dengue relative risks can be precisely modeled, and the prediction distribution can also capture the observed RR during the testing periods. It should be noted that the predictive uncertainty is positively asymmetric due to the asymmetric nature of relative risks and the model contemplates the log of relative risks.

For the spatial dimension, Figure 6 presents the posterior predictive dengue relative risk

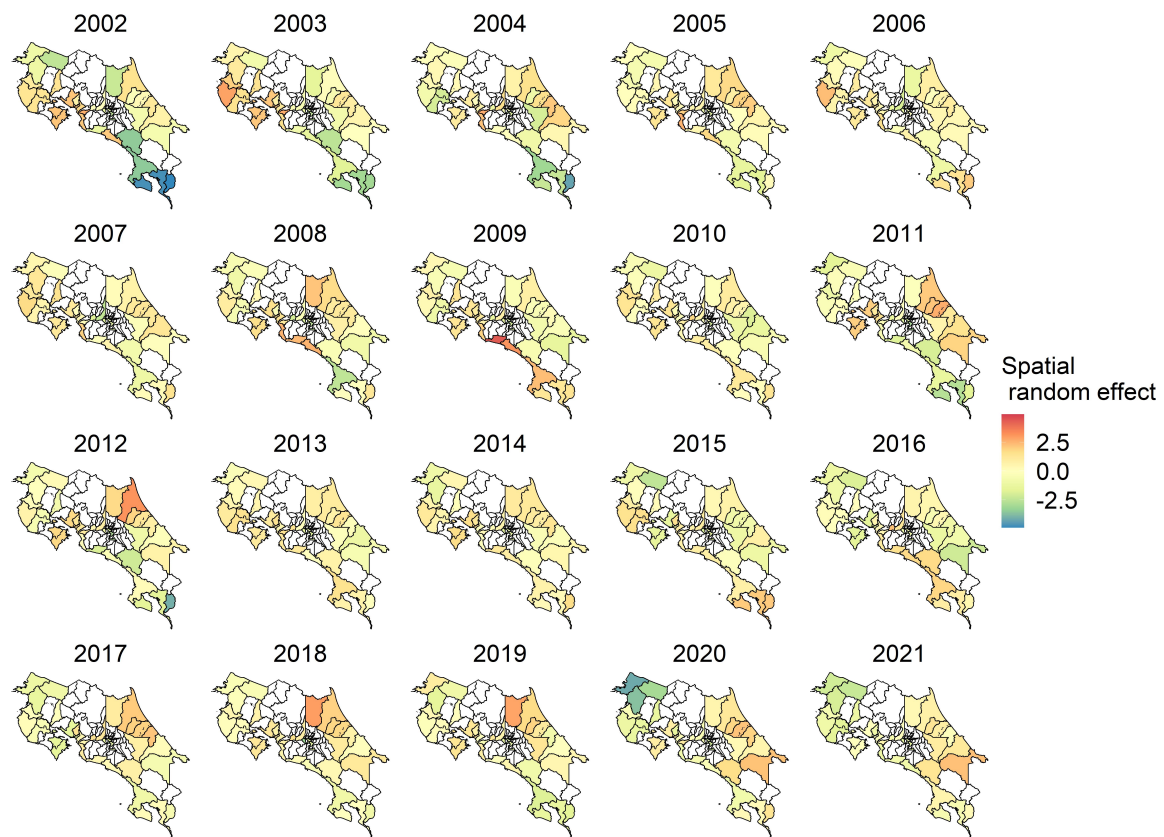


Figure 3: Contribution of year-specific spatial random effect to dengue log relative risk.

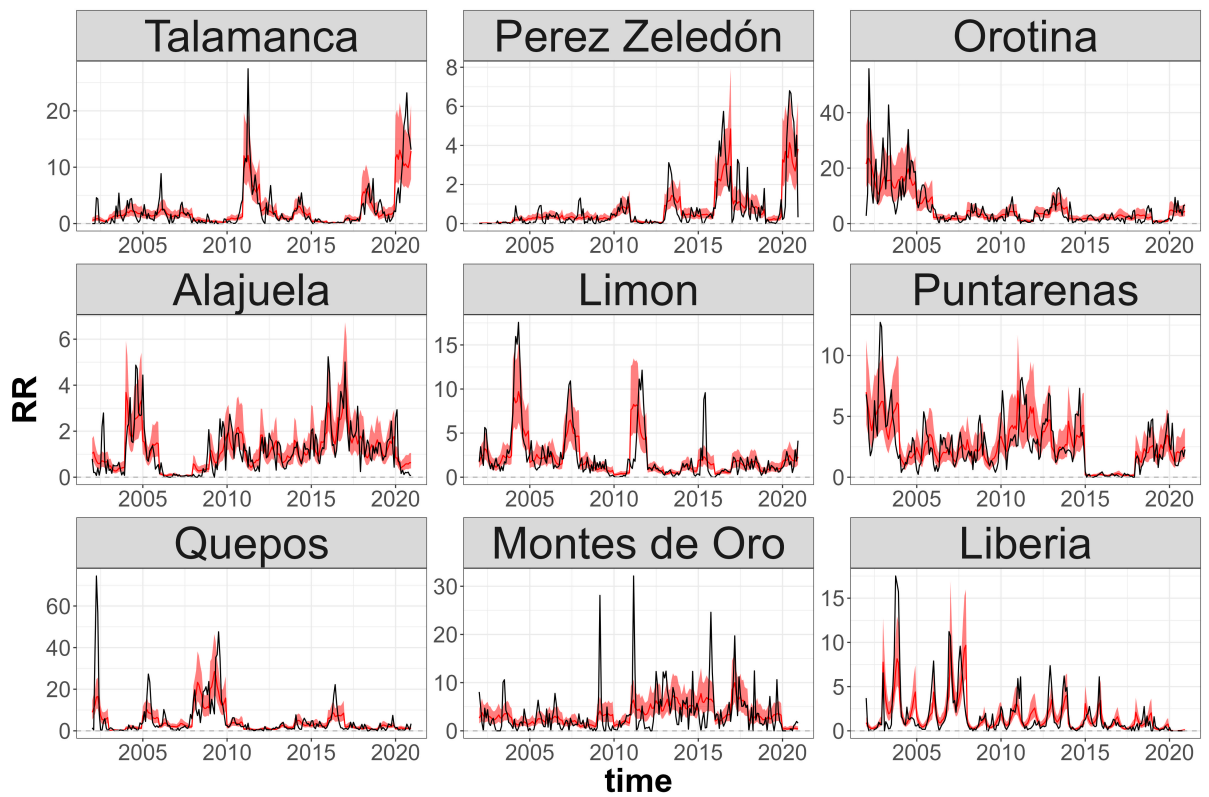


Figure 4: Observed (black) and 95% posterior predictive dengue relative risks (red) over the training period. Upper six panels: best municipalities according to NIS metric. Lower three panels: worst municipalities according to NIS metric.

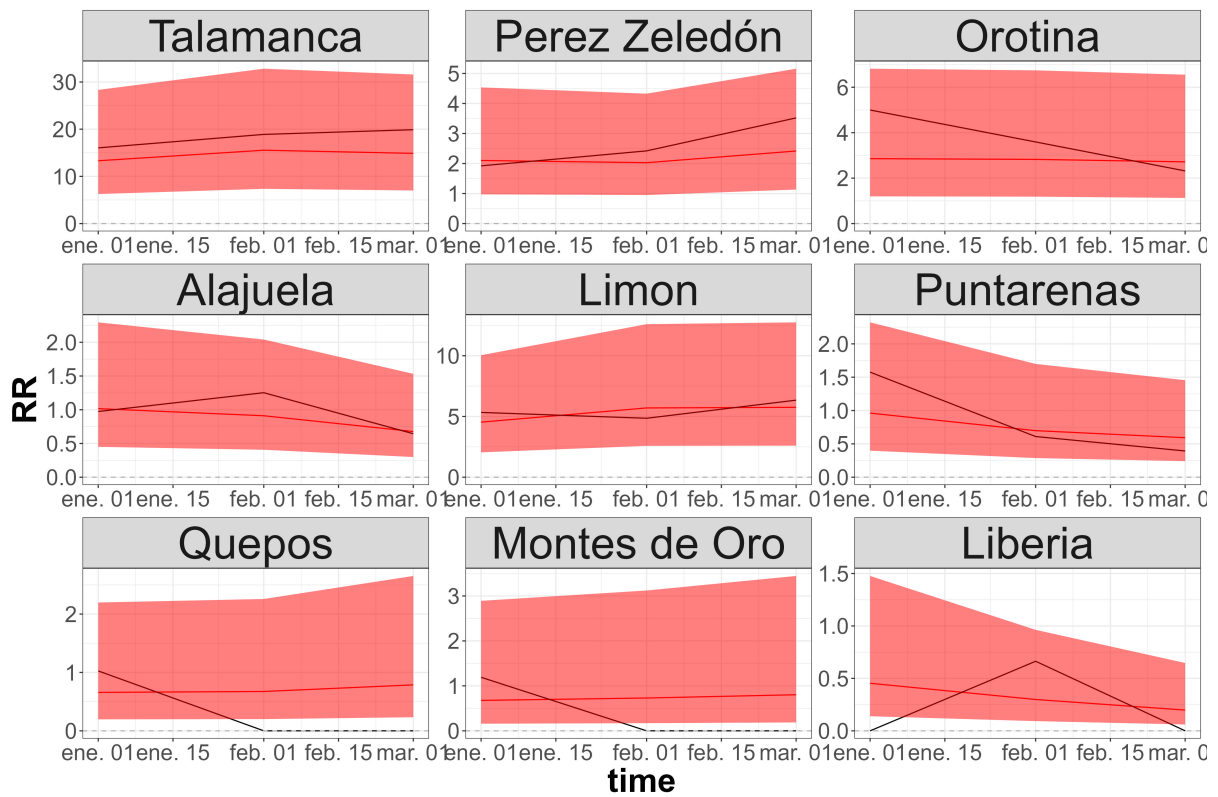


Figure 5: Observed (black) and 95% posterior predictive dengue relative risks (red) over the testing period. Upper six panels: best municipalities according to NIS metric. Lower three panels: worst municipalities according to NIS metric.

mean and their absolute percentage error for each municipality and month (January, February, and March). These maps allow us to visualize regions with higher dengue relative risks in a specific month. Furthermore, Figure 6b shows that the absolute percentage error is uniform across the region for the testing period.

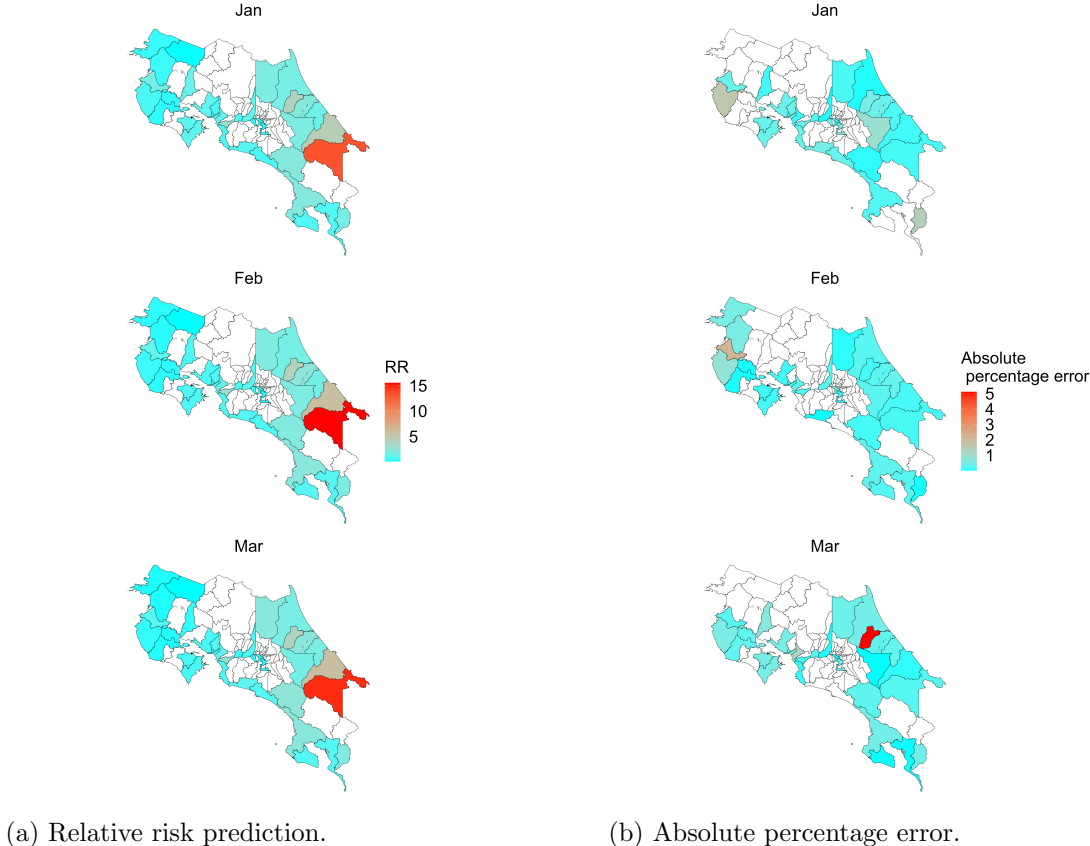


Figure 6: Relative risk prediction and their absolute percentage error from January to March 2020 for 81 municipalities in Costa Rica.

For the training set, similar behavior is visualized. Maps of the posterior mean of relative risks for three selected years (2002, 2011, 2020) and maps of absolute percentage error for the same years are shown in Sections C and D of the Supplementary Material.

4 Discussion

Epidemiological models provide a crucial tool to help public health authorities and policy-makers to allocate limited resources effectively and efficiently. Using these predictive models helps understand disease dynamics, the potential impact on the population, and the health system’s response to an outbreak. These models can be improved by including demographics, genetics, and environmental variables to make more accurate predictions.

One of the challenges in developing and using epidemiological models is obtaining high-quality data. A robust and comprehensive data collection system is essential to provide accurate input for the models. In addition, the data must be integrated and processed consistently and timely to ensure that the models are accurate and up-to-date. Data sources

include health records, laboratory results, surveillance systems, and household surveys. The output of these models can help in decision-making processes concerning control purposes and surveillance methods and hopefully also as good predictive tools. Prediction forms part of surveillance systems, and more specifically in early warning systems [43].

The effect of climate variability and climate change on dengue transmission is complex, nonlinear, and often delayed by several weeks to months [13, 44]. Bringing together spatio-temporal patterns of dengue transmission compatible with long-term data on climate and other socio-ecological changes in mathematical and statistical models could improve projections of dengue risks and disease control.

Based on the results of fitting the model (1) to the dengue data, it is clear that incorporating all climate covariates greatly improved the model's performance in accurately predicting the number of dengue cases. Using different structures in the model allowed for a deeper understanding of the relationships between dengue transmission and climate factors. The model's results demonstrate its potential to be a useful tool for decision-making processes in disease control and surveillance methods. Furthermore, the successful application of the model to monthly data from January 2000 to March 2021 highlights its potential for future predictions and early warning systems.

The spatio-temporal random components in the model make us aware that more structural information, such as human mobility and socio-economic factors, could be considered to obtain better predictive results. Access to these data is challenging, and we are working on it in future investigations.

Finally, by providing accurate predictions, decision-makers can respond more effectively to outbreaks and implement strategies to reduce the impact of the disease on the population. Thus, helping health authorities optimize the typically scarce resources. To maximize their effectiveness, models must be based on high-quality data, continuously updated, and validated jointly with public health officials to reflect environmental changes and other factors, including social determinants, that may impact disease transmission. The continued development of these models will play a critical role in the fight against dengue and other infectious diseases.

References

- [1] World Health Organization (WHO). Dengue and severe dengue, August 2022.
- [2] Jolyon M Medlock, David Avenell, Iain Barrass, and Steve Leach. Analysis of the potential for survival and seasonal activity of *Aedes albopictus* (Diptera: Culicidae) in the United Kingdom. *Journal of Vector Ecology*, 31(2):292–304, 2006.
- [3] Roberto Romi, Francesco Severini, and Luciano Toma. Cold acclimation and overwintering of female *Aedes albopictus* in Roma. *Journal of the American Mosquito Control Association*, 22(1):149–151, 2006.
- [4] Abdelkrim Outammassine, Said Zouhair, and Souad Loqman. Global potential distribution of three underappreciated arboviruses vectors (*Aedes japonicus*, *Aedes vexans* and *Aedes vittatus*) under current and future climate conditions. *Transboundary and Emerging Diseases*, 69(4):e1160–e1171, 2022.
- [5] Natasha Evelyn Anne Murray, Mikkel B Quam, and Annelies Wilder-Smith. Epidemiology of dengue: past, present and future prospects. *Clinical epidemiology*, 5:299, 2013.

- [6] Eduardo Massad, Marcos Amaku, Francisco Antonio Bezerra Coutinho, Claudio José Struchiner, Marcelo Nascimento Burattini, Kamran Khan, Jing Liu-Helmerson, Joacim Rocklöv, Moritz UG Kraemer, and Annelies Wilder-Smith. Estimating the probability of dengue virus introduction and secondary autochthonous cases in europe. *Scientific reports*, 8(1):1–12, 2018.
- [7] Luis Fernandez Lopez, Marcos Amaku, Francisco Antonio Bezerra Coutinho, Mikkel Quam, Marcelo Nascimento Burattini, Claudio José Struchiner, Annelies Wilder-Smith, and Eduardo Massad. Modeling importations and exportations of infectious diseases via travelers. *Bulletin of mathematical biology*, 78(2):185–209, 2016.
- [8] Duane J Gubler. The economic burden of dengue. *The American journal of tropical medicine and hygiene*, 86(5):743, 2012.
- [9] Hao Wang, Shaohua Zhao, Shengjun Wang, Yue Zheng, Shaohua Wang, Hui Chen, Jiaojiao Pang, Juan Ma, Xiaorong Yang, and Yuguo Chen. Global magnitude of encephalitis burden and its evolving pattern over the past 30 years. *Journal of Infection*, 84(6):777–787, 2022.
- [10] Jane P Messina, Oliver J Brady, Nick Golding, Moritz UG Kraemer, GR Wint, Sarah E Ray, David M Pigott, Freya M Shearer, Kimberly Johnson, Lucas Earl, et al. The current and future global distribution and population at risk of dengue. *Nature microbiology*, 4(9):1508–1515, 2019.
- [11] Xiaorong Yang, Mikkel BM Quam, Tongchao Zhang, and Shaowei Sang. Global burden for dengue and the evolving pattern in the past 30 years. *Journal of travel medicine*, 28(8):taab146, 2021.
- [12] Cory W Morin, Andrew C Comrie, and Kacey Ernst. Climate and dengue transmission: evidence and implications. *Environmental health perspectives*, 121(11-12):1264–1272, 2013.
- [13] Suchithra Naish, Pat Dale, John S Mackenzie, John McBride, Kerrie Mengersen, and Shilu Tong. Climate change and dengue: a critical and systematic review of quantitative modelling approaches. *BMC infectious diseases*, 14(1):1–14, 2014.
- [14] Karen M Campbell, Kristin Haldeman, Chris Lehnig, Cesar V Munayco, Eric S Halsey, V Alberto Laguna-Torres, Martín Yagui, Amy C Morrison, Chii-Dean Lin, and Thomas W Scott. Weather regulates location, timing, and intensity of dengue virus transmission between humans and mosquitoes. *PLoS neglected tropical diseases*, 9(7):e0003957, 2015.
- [15] Douglas M Watts, Donald S Burke, Bruce A Harrison, Richard E Whitmire, and Ananda Nisalak. Effect of temperature on the vector efficiency of aedes aegypti for dengue 2 virus. Technical report, ARMY MEDICAL RESEARCH INST OF INFECTIOUS DISEASES FORT DETRICK MD, 1986.
- [16] W Tun-Lin, TR Burkot, and BH Kay. Effects of temperature and larval diet on development rates and survival of the dengue vector aedes aegypti in north queensland, australia. *Medical and veterinary entomology*, 14(1):31–37, 2000.

- [17] LM Rueda, KJ Patel, RC Axtell, and RE Stinner. Temperature-dependent development and survival rates of *Culex quinquefasciatus* and *Aedes aegypti* (Diptera: Culicidae). *Journal of medical entomology*, 27(5):892–898, 1990.
- [18] Muhammad Shahzad Sarfraz, Nitin K Tripathi, Taravudh Tipdecho, Thawisak Thongbu, Pornsuk Kerdthong, and Marc Souris. Analyzing the spatio-temporal relationship between dengue vector larval density and land-use using factor analysis and spatial ring mapping. *BMC public health*, 12(1):1–19, 2012.
- [19] Hamady Dieng, Abu Hassan Ahmad, Jazem A Mahyoub, Abdulhafis M Turkistani, Hatabbi Mesed, Salah Koshike, Tomomitsu Satho, MR Che Salmah, Hamdan Ahmad, Wan Fatma Zuharah, et al. Household survey of container–breeding mosquitoes and climatic factors influencing the prevalence of *Aedes aegypti* (Diptera: Culicidae) in Makkah city, Saudi Arabia. *Asian Pacific journal of tropical biomedicine*, 2(11):849–857, 2012.
- [20] Birgit HB Van Benthem, Sophie O Vanwambeke, Nardlada Khantikul, Chantal Burghoorn-Maas, Kamolwan Panart, Linda Oskam, Eric F Lambin, and Pradya Somboon. Spatial patterns of and risk factors for seropositivity for dengue infection. *The American journal of tropical medicine and hygiene*, 72(2):201–208, 2005.
- [21] Roberto Barrera, Manuel Amador, and Gary G Clark. Ecological factors influencing *Aedes aegypti* (Diptera: Culicidae) productivity in artificial containers in Salinas, Puerto Rico. *Journal of medical entomology*, 43(3):484–492, 2006.
- [22] Julio César Mateus and Gabriel Carrasquilla. Predictors of local malaria outbreaks: an approach to the development of an early warning system in Colombia. *Memórias do Instituto Oswaldo Cruz*, 106:107–113, 2011.
- [23] Millicent Eidson, Laura Kramer, Ward Stone, Yoichiro Hagiwara, Kate Schmit, New York State West Nile Virus Avian Surveillance Team, et al. Dead bird surveillance as an early warning system for West Nile virus. *Emerging infectious diseases*, 7(4):631, 2001.
- [24] European Centre for Disease Prevention and Control. Vboret–European network for arthropod vector surveillance for human public health, August 2022.
- [25] Ministerio de Salud. Sitio web del ministerio de salud de Costa Rica. bienvenido, 2022.
- [26] Paola Vásquez, Antonio Loría, Fabio Sanchez, and Luis A. Barboza. Climate-driven Statistical Models as effective predictors of local Dengue incidence in Costa Rica: a Generalized Additive Model and Random Forest Approach. *Revista de Matemática: Teoría y Aplicaciones*, 27(1):1–21, 2020.
- [27] Yury E. Garcia, Shu-Wei Chou-Chen, Luis A. Barboza, Maria L. Daza-Torres, J. Cricelio Montesinos-Lopez, Paola Vasquez, Juan G. Calvo, Miriam Nuno, and Fabio Sanchez. Common patterns between dengue cases, climate, and local environmental variables in Costa Rica: A wavelet approach, 2023.
- [28] Ministerio de Salud. Sitio web del ministerio de salud de Costa Rica. bienvenido, 2022.
- [29] Chris Funk, Pete Peterson, Martin Landsfeld, Diego Pedreros, James Verdin, Shradhanand Shukla, Gregory Husak, James Rowland, Laura Harrison, Andrew Hoell, and

- Joel Michaelsen. The climate hazards infrared precipitation with stations—a new environmental record for monitoring extremes. *Scientific data*, 2(1):150066–150066, 2015.
- [30] NOAA. Climate prediction center. <https://www.cpc.ncep.noaa.gov/data/indices/ersst5.nino.mth.91-20.ascii>. Accessed: 2022-05-01.
- [31] Sean L. Tuck, Helen R.P. Phillips, Rogier E. Hintzen, Jörn P.W. Scharlemann, Andy Purvis, and Lawrence N. Hudson. Modistools – downloading and processing modis remotely sensed data in r. *Ecology and Evolution*, 4(24):4658–4668, 2014.
- [32] David B Enfield, Alberto M Mestas-Nuñez, Dennis A Mayer, and Luis Cid-Serrano. How ubiquitous is the dipole relationship in tropical atlantic sea surface temperatures? *Journal of Geophysical Research: Oceans*, 104(C4):7841–7848, 1999.
- [33] H G Hidalgo, E J Alfaro, and B Quesada-Montano. Observed (1970–1999) climate variability in central america using a high-resolution meteorological dataset with implication to climate change studies. *Clim. Change*, 141(1):13–28, 2017.
- [34] A. Gasparrini, B. Armstrong, and M. G. Kenward. Distributed lag non-linear models. *Statistics in Medicine*, 29(21):2224–2234, 2010.
- [35] Antonio Gasparrini. Modeling exposure–lag–response associations with distributed lag non-linear models. *Statistics in Medicine*, 33(5):881–899, 2014.
- [36] Julian Besag, Jeremy York, and Annie Mollié. Bayesian image restoration, with two applications in spatial statistics. *Annals of the Institute of Statistical Mathematics*, 43(1):1–20.
- [37] Roger Bivand, Virgilio Gómez-Rubio, and Håvard Rue. Spatial data analysis with r-inla with some extensions. *Journal of Statistical Software*, 63(20):1–31, 2015.
- [38] A. Gasparrini. Distributed lag linear and non-linear models in R: the package dlnm. *Journal of Statistical Software*, 43(8):1–20, 2011.
- [39] Håvard Rue, Sara Martino, and Nicolas Chopin. Approximate Bayesian Inference for Latent Gaussian Models by Using Integrated Nested Laplace Approximations. *Journal of the Royal Statistical Society . Series B (Methodological)*, 71(2):319–392, 2009.
- [40] Luis A. Barboza, Shu-Wei Chou-Chen, Paola Vásquez, Yury E. García, Juan G. Calvo, Hugo G. Hidalgo, and Fabio Sanchez. Assessing dengue fever risk in costa rica by using climate variables and machine learning techniques. *PLOS Neglected Tropical Diseases*, 17(1):1–13, 01 2023.
- [41] Robert L Winkler and Allan H Murphy. “Good” Probability Assessors. *Journal of Applied Meteorology and Climatology*, 7(5):751–758, 1968.
- [42] Tilmann Gneiting and Adrian E Raftery. Strictly Proper Scoring Rules, Prediction, and Estimation. *Journal of the American Statistical Association*, 102(477):359–378, mar 2007.
- [43] Vanessa Racloz, Rebecca Ramsey, Shilu Tong, and Wenbiao Hu. Surveillance of dengue fever virus: a review of epidemiological models and early warning systems. *PLoS neglected tropical diseases*, 6(5):e1648, 2012.

- [44] Tzai-Hung Wen, Neal H Lin, Chun-Hung Lin, Chwan-Chuen King, and Ming-Daw Su. Spatial mapping of temporal risk characteristics to improve environmental health risk identification: a case study of a dengue epidemic in taiwan. *Science of the Total Environment*, 367(2-3):631–640, 2006.

**Supplemental Materials: Bayesian spatio-temporal model with INLA for
dengue fever risk prediction in Costa Rica**

A Naïve methods' predictive metrics of the testing period (from January to March 2021)

Table A.1: Predictive metrics of testing data set of the naïve forecasting and negative binomial null model

Municipality	Naive method	Negative Binomial null model	
	<i>NRMSE</i>	<i>NRMSE</i>	<i>NIS</i> ₉₅
Alajuela	2.6506	1.4229	42.9843
Alajuelita	0.4765	2.1888	59.8866
Atenas	89.8765	7.3082	156.7569
Cañas	3.5234	2.9727	69.7955
Carrillo	0.8118	0.9751	26.7633
Corredores	0.3051	0.7459	20.5897
Desamparados	0.2598	22.3581	436.3609
Esparza	0.6795	0.9124	26.0958
Garabito	15.6450	9.0487	189.7400
Golfoito	0.9871	3.6079	82.9118
Guacimo	3.6451	3.2932	28.8848
La Cruz	3.5519	17.4492	339.4951
Liberia	0.4927	16.3574	319.1370
Limon	3.4131	2.1836	23.9121
Matina	2.6768	0.8195	30.0298
Montes de Oro	41.8550	8.0778	160.1058
Nicoya	9.2749	17.0730	338.3457
Orotina	2.2117	0.9807	15.6226
Osa	1.2030	0.6291	13.9754
Parrita	15.7029	2.4511	54.8356
Perez Zeledón	1.5211	0.2745	7.9940
Pococí	1.0359	0.2630	10.7672
Puntarenas	0.7206	2.0884	52.3785
Quepos	10.8189	9.6902	192.1924
San Jose	0.0267	11.4795	237.4494
Santa Ana	0.4281	19.8108	383.3144
SantaCruz	2.3943	6.6282	144.8392
Sarapiquí	13.7461	0.0603	3.2807
Siquirres	1.8468	0.2815	9.1988
Talamanca	13.8805	14.4673	35.1501
Turrialba	1.4088	0.3812	14.9645
Upala ¹	-	-	-

¹ *NRMSE* and *NIS*₉₅ for Upala is not shown since the observed relative risks are zero.

B Dengue cases modelling and prediction

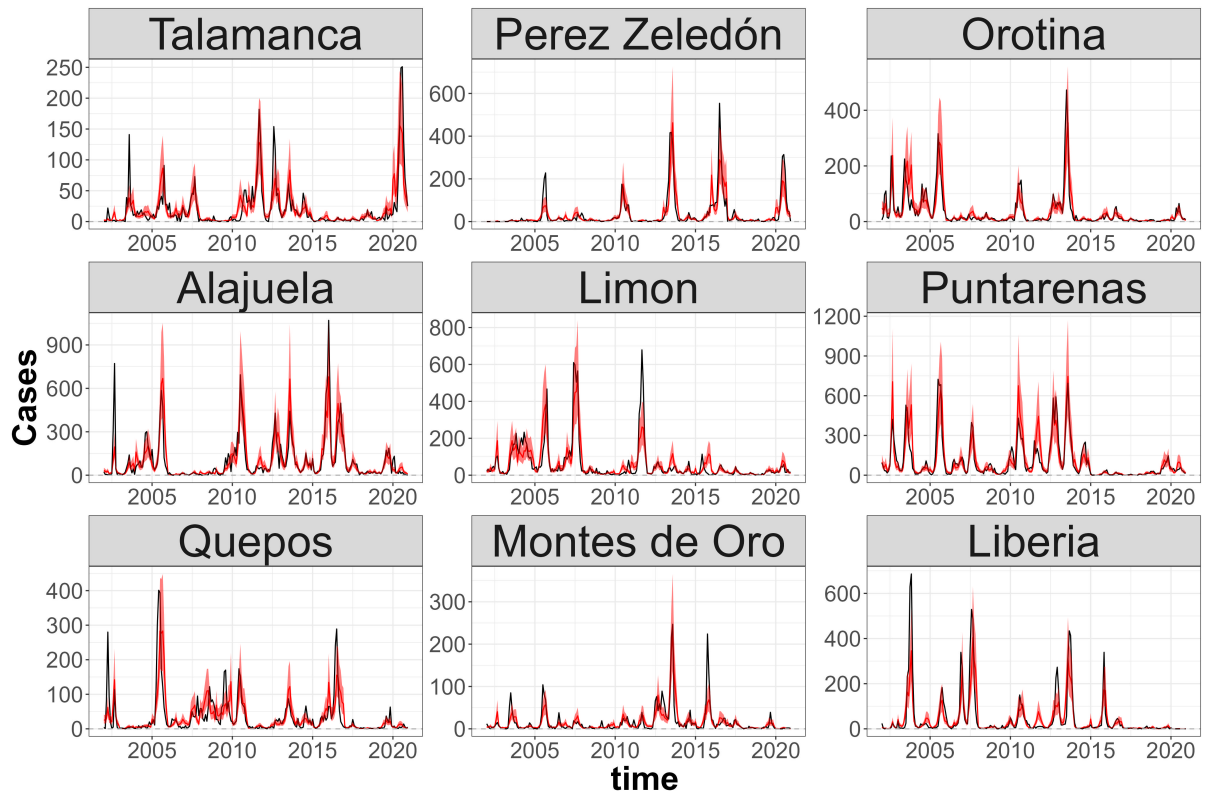


Figure B.1: Observed (black) and 95% posterior predictive dengue cases (red) over the training period. Upper six panels: best municipalities according to NIS metric. Lower three panels: worst municipalities according to NIS metric.

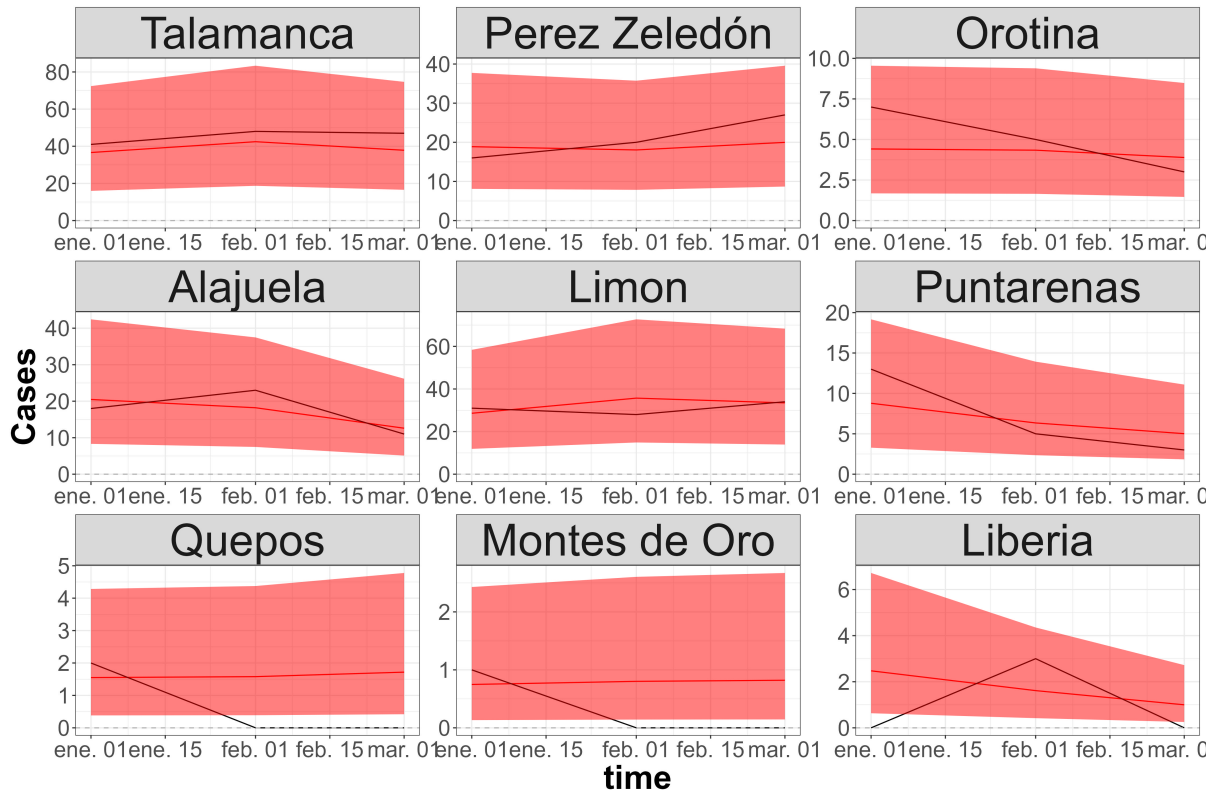


Figure B.2: Observed (black) and 95% posterior predictive dengue cases (red) over the testing period. Upper six panels: best municipalities according to NIS metric. Lower three panels: worst municipalities according to NIS metric.

C Relative risk prediction maps in 2002, 2011 and 2020

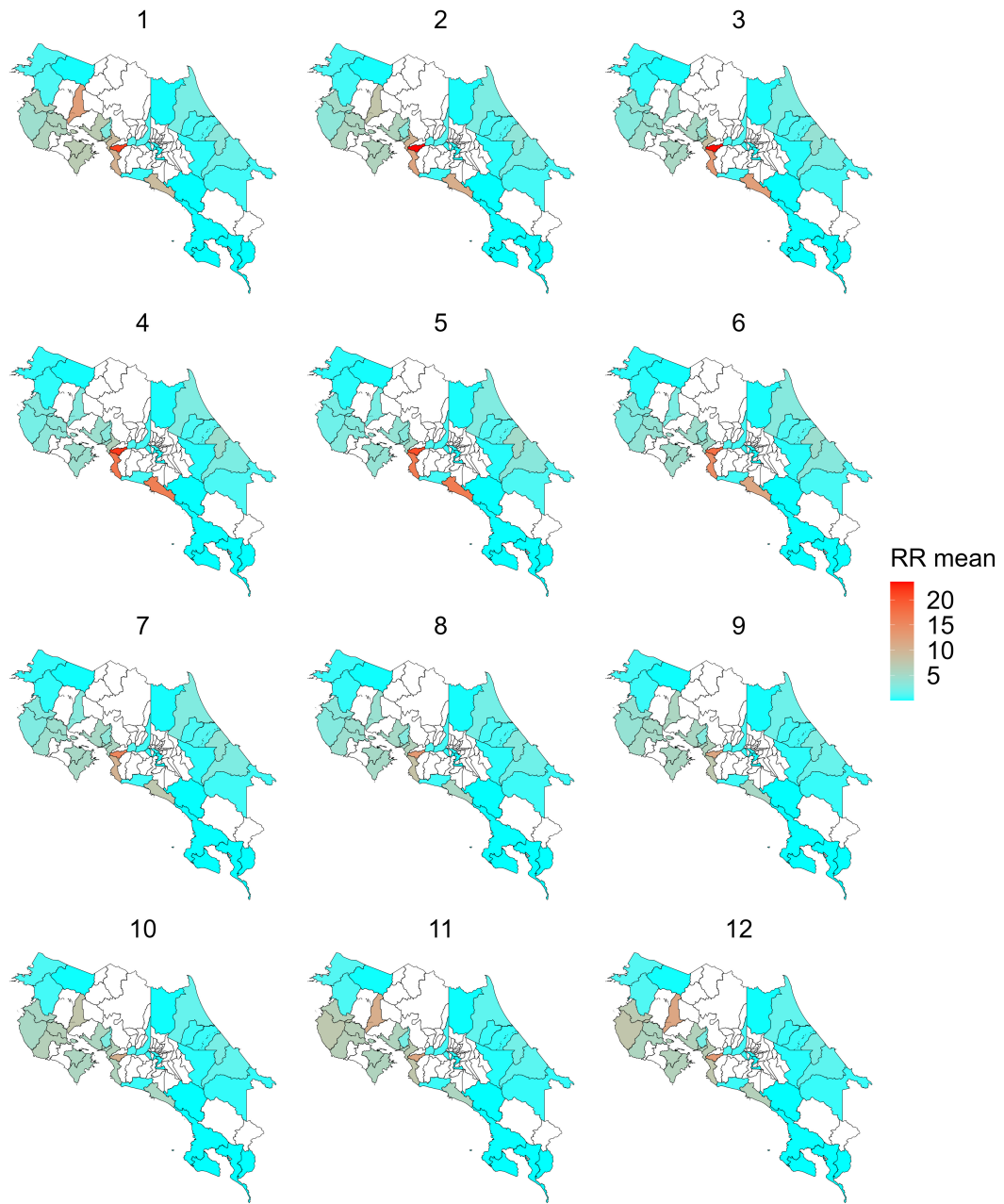


Figure C.1: Posterior mean of relative risks from January to December 2002 for 81 municipalities in Costa Rica.

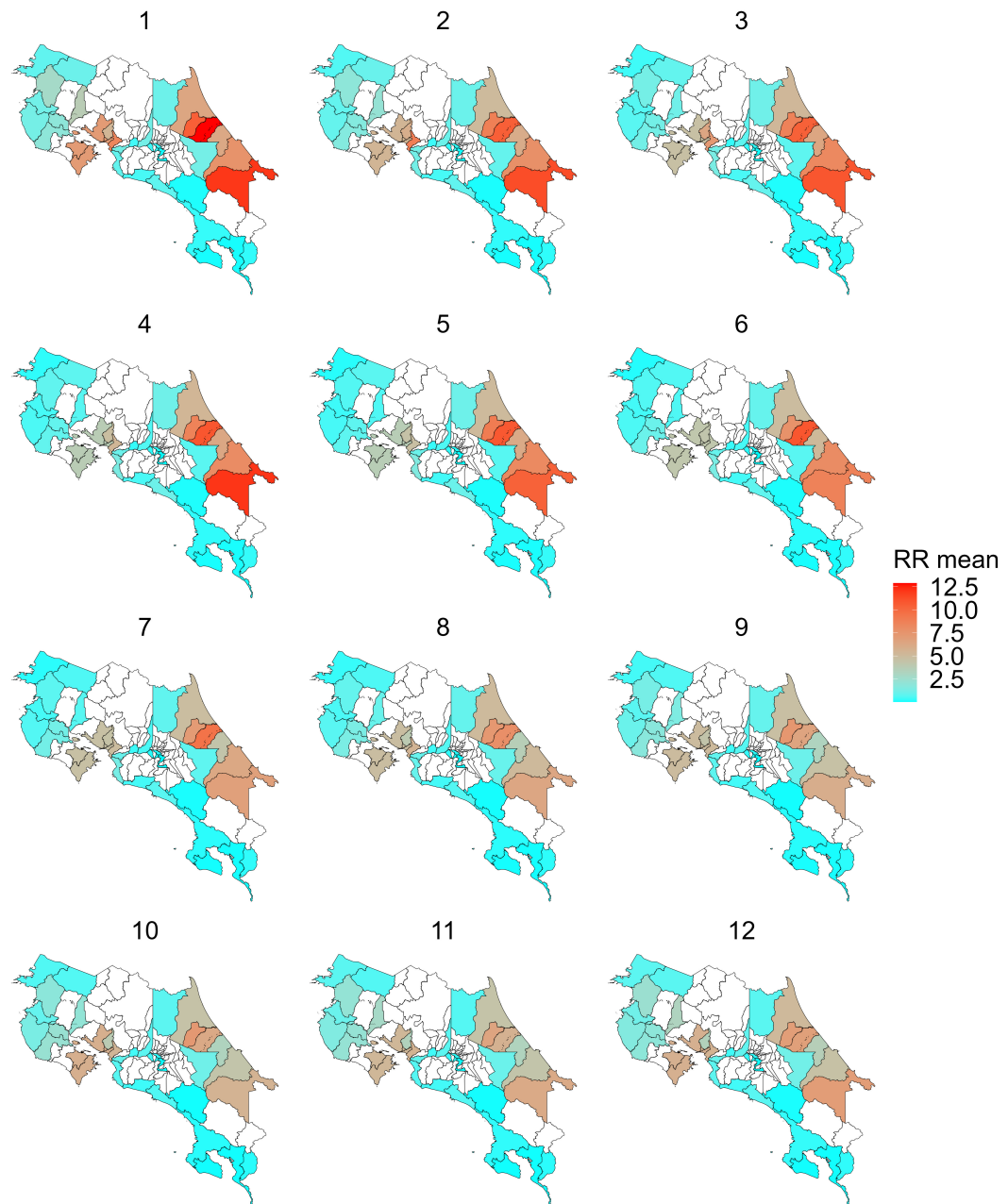


Figure C.2: Posterior mean of relative risks from January to December 2011 for 81 municipalities in Costa Rica.

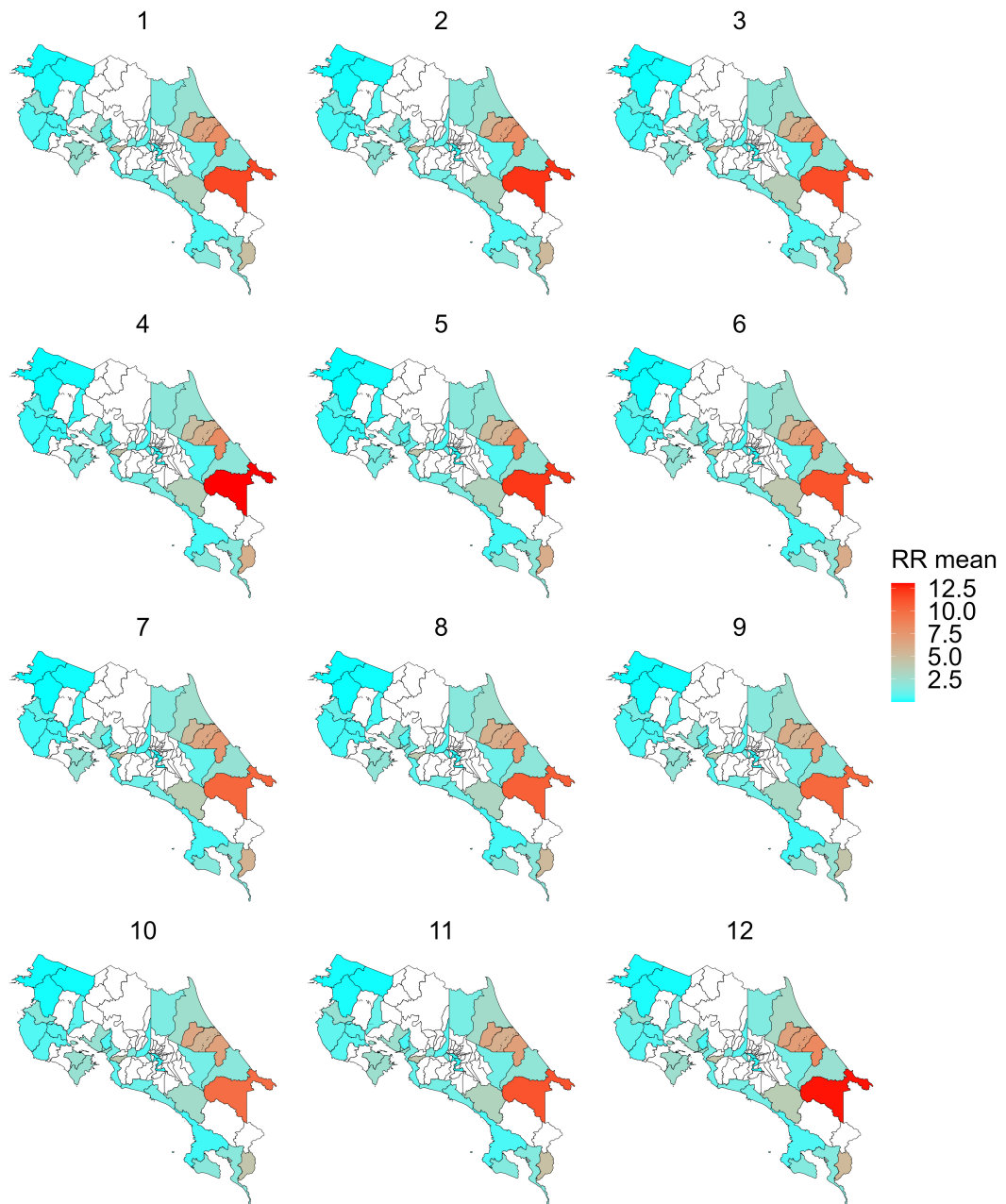


Figure C.3: Posterior mean of relative risks from January to December 2020 for 81 municipalities in Costa Rica.

D Absolute percentage error maps in 2002, 2011 and 2020

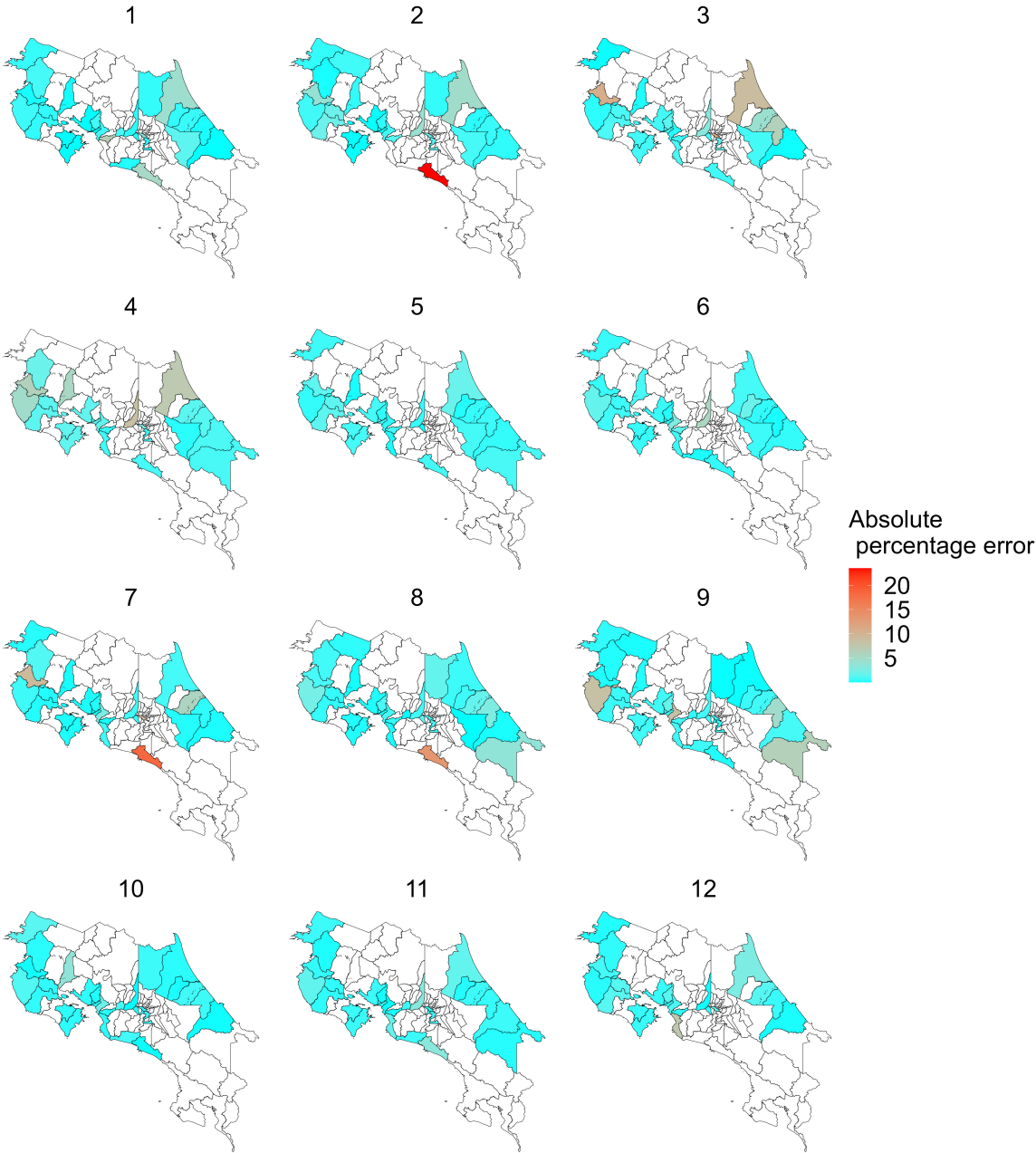


Figure D.1: Absolute percentage error from January to December 2002 for 81 municipalities in Costa Rica.

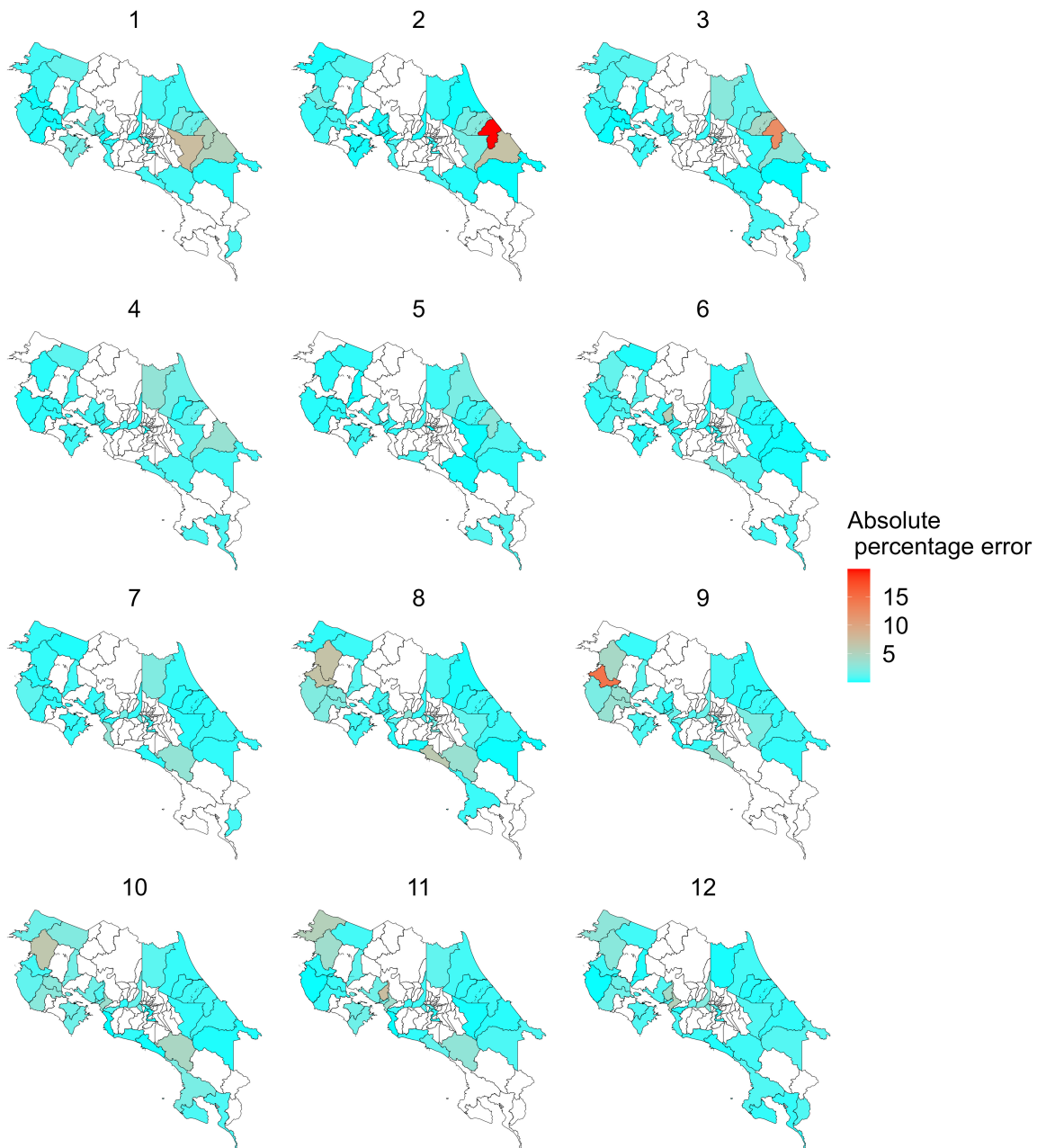


Figure D.2: Absolute percentage error from January to December 2011 for 81 municipalities in Costa Rica.

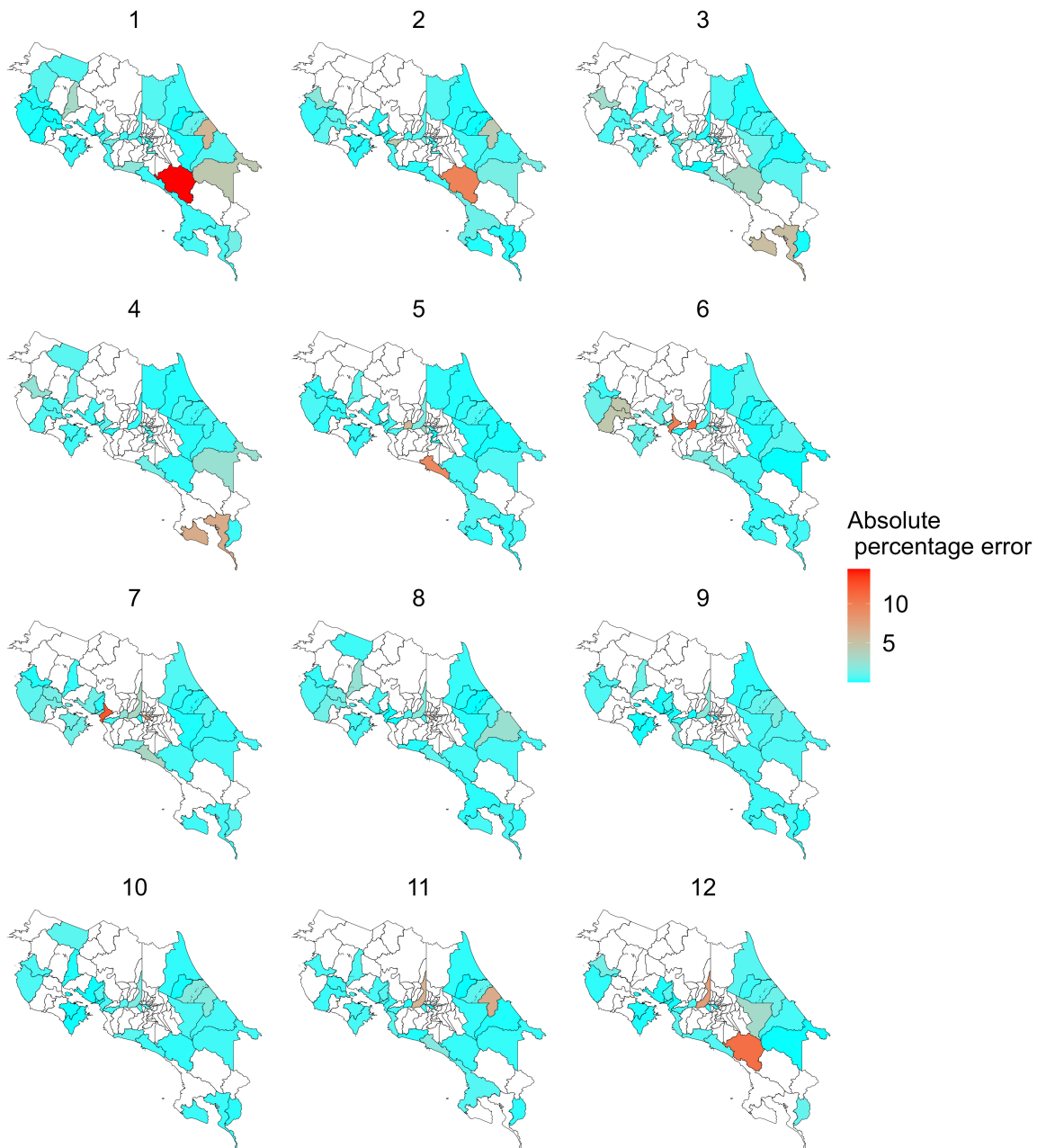


Figure D.3: Absolute percentage error from January to December 2020 for 81 municipalities in Costa Rica.